

# Monte-Carlo Simulation of $\gamma$ -ray and Fast Neutron Radiolysis of Liquid Water and 0.4 M $H_2SO_4$ Solutions at Temperatures up to 325°C

G.R. Sunaryo<sup>1,2\*</sup>, M. Jintana<sup>1</sup> and J.P.J. Gerin<sup>1</sup>

<sup>1</sup>Département de Médecine Nucléaire et de Radiobiologie, Faculté de Médecine et des Sciences de la Santé, Université de Sherbrooke (Québec) J1H 5N4, Canada

<sup>2</sup>Center for Reactor Technology and Nuclear Safety, National Nuclear Energy Agency Puspptek, Serpong, Tangerang 15310, Indonesia

## ARTICLE INFO

### Article history:

Received 20 November 2009

Received in Revised form 06 April 2011

Accepted 12 April 2011

### Keywords:

Monte-Carlo  
 $\gamma$ -Radiolysis  
Fast neutrons

## ABSTRACT

Monte-Carlo simulations were used to study the radiolysis of liquid water at 25-325°C when subjected to low linear energy transfer (LET) of  $^{60}Co$   $\gamma$ -ray radiation and fast neutrons of 2 and 0.8 MeV. The energy deposited in the early stage of  $^{60}Co$   $\gamma$ -ray irradiation was approximated by considering short segments (~150  $\mu m$ ) of 300 MeV proton tracks, corresponding to an average LET of ~0.3 keV/ $\mu m$ . In case of 2 MeV fast neutrons, the energy deposited was considered by using short segments (~5  $\mu m$ ) of energy at 1.264, 0.465, 0.171, 0.063 and 0.24 MeV. 0.8 MeV fast neutrons were approximated by 0.505, 0.186, 0.069 and 0.025 MeV protons. The effect of 0.4 M  $H_2SO_4$  solution on radiolysis was also studied by this method for both  $^{60}Co$   $\gamma$ -rays and 0.8 MeV fast neutrons. The simulated results at the time of  $10^{-7}$ s after irradiation were obtained and compared with the available experimental results published by other researchers to be in excellent agreement with them over the entire temperature ranges and radiation sources studied. Except for  $g(H_2)$  that increase with temperature rises, the general behaviors of higher radical products and lower molecular products at higher temperatures were obtained. The LET effect is also validated by this study, showing that the increase in LET would yield higher molecular and lower radical products. Studies on 0.4 M  $H_2SO_4$  solutions also show good agreement between the computed and experimental data for  $\gamma$ -ray irradiation: the presence of 0.4 M  $H^+$ , except for  $g(H_2)$  that gives lower value at 25°C and higher value at 325°C, gives the higher values for radicals and  $g(H_2O_2)$  at 25°C and lower values at 325°C, compared with that for neutral water. The computed data show good agreement with the experimental data for 0.4 M  $H_2SO_4$  solutions induced by 0.8 MeV fast neutrons, except for  $g(H_2)$  and  $g(H^\bullet)$  that gives good agreement up to 50°C, then the opposite tendencies with the further temperature rises. However, the simulated fast neutron radiolysis on acidic demonstrates similar tendencies on temperature dependence with that for simulated  $^{60}Co$   $\gamma$ -radiolysis, but in different magnitude. For better understanding, more experimental data for fast neutrons are needed, especially under the acidic conditions.

© 2011 Atom Indonesia. All rights reserved

## INTRODUCTION

The elucidation of the mechanism of water radiolysis, is interesting scientifically, especially at the early time of the process, time scale  $\sim 10^{-7}$ s. Many theoretical studies have been conducted by a spur diffusion model which facilitates the dependence of the yields of radiolytic products on the solute concentration and on LET (linear energy transfer) by changing the spur interval. The

stochastic methods such as Monte Carlo simulations was originally used to simulate the physical stage in water radiolysis, then applied to the simulation of physico-chemical or chemical stage. J.-P. Jay-Gerin group has been developing the Monte-Carlo computer code for simulating the radiolytic product from various aspects through the temperature dependence observation of primary radical ( $e_{aq}^-$ ,  $H^\bullet$  and  $\bullet OH$ ) and molecular ( $H_2$  and  $H_2O_2$ ) yields (or  $g$ -values pertaining to the yields of species of each kind, expressed in units of particles per 100 eV of absorbed energy which escape from the

\* Corresponding author.  
E-mail address: genirina@batan.go.id

spurs  $\sim 10^{-7}$ s after irradiation at 25°C and become distributed homogeneously in the bulk of the solution of the radiolysis of pure, deaerated liquid water) [1]. The computed data shows relatively good agreement with the existing experimental data. This code was also used to calculate the yields induced by the high LET radiation of 6 MeV  $^2\text{H}^+$ , 0.215 MeV  $^1\text{H}^+$  and 40 MeV  $^7\text{Li}^{3+}$  ions, for which the LET values at 25°C are  $\sim 11.7$ , 63.5 and 63.8 keV/ $\mu\text{m}$ , respectively [2].

In this paper, the Monte-Carlo simulation code was used to understand the behavior of radiolysis products under fast neutron irradiation up to temperature  $\sim 325^\circ\text{C}$  for both neutral water and 0.4 M  $\text{H}_2\text{SO}_4$  solutions at the early time  $\sim 10^{-7}$ s. The code was verified first for neutral water at 25–325°C when subjected to  $^{60}\text{Co}$   $\gamma$ -rays, and then applied to fast neutrons at 2 and 0.8 MeV. Good agreement between simulated and experimental data was obtained, and then the code was applied to study the effect of 0.4 M  $\text{H}_2\text{SO}_4$  under both of  $^{60}\text{Co}$   $\gamma$ -rays and 0.8 MeV fast neutrons. The computed data were acquired at the time of observation at  $10^{-7}$ s and verified against the existing experimental data.

## EXPERIMENTAL METHODS

### Monte-Carlo Simulation

The detailed description of present Monte-Carlo modeling for radiolysis of liquid water has been written elsewhere [1-10]. To reproduce the effect of  $^{60}\text{Co}$   $\gamma$ -ray radiolysis and fast electrons, 150 ions,  $\sim 150\mu\text{m}$  short track segments of 300MeV protons (where the average LET value obtained by the simulations is  $\sim 0.3$  keV/ $\mu\text{m}$  at 25°C, which is similar to the LET of  $^{60}\text{Co}$   $\gamma$ -ray) [11] and end track length of 0.5–1.5 $\mu\text{m}$  for temperature range of 25–325 °C were applied. However, the effect of fast neutron irradiation was simulated with less exhausted data inputs, i.e. 10 ions, 1.5  $\mu\text{m}$  track length and 1.5  $\mu\text{m}$  end track length. This analysis gives the track segment yields at a well-defined LET. The proton energy used for reproducing the primary yields from 2 and 0.8 MeV fast neutrons irradiation will be discussed later.

### Thermalization distance

Thermalization distance ( $r_{\text{th}}$ ) of subexcitation electrons [4,12-14] at 300°C (the transport of excitation electrons in water from their initial energies until they become thermalized,  $\sim 7.3$  eV in

liquids water), was adjusted by the previous author to bring the present simulation results and their computed data into good concurrence. The corrected primary yields were  $e_{\text{aq}}^-$  and  $\text{H}^\bullet$ . As a result, the  $r_{\text{th}}$  value of  $\frac{r_{\text{th}} 25^\circ\text{C}}{2}$  at 300°C was applied for all simulation studies in this paper, including the solutions and initial incident proton energy at present work [1].

### Time scale

$10^{-7}$ s time dependent were acquired which is the elapsed time after irradiation at which the homogeneous chemistry is presumed to start taking place all over at high temperatures up to  $\sim 325^\circ\text{C}$ .

## Reaction Scheme

### For neutral solution

The scheme of reactions used for the present work to reproduce the primary yields as a function of temperature up to 325°C has been reported elsewhere [1-2]. Some additional reactions were introduced here and the recent values of rate constant were also applied for the present simulations. The recent reported values of rate constant as a function of temperature were applied directly, wherever appropriate, but some reactions with unknown temperature dependence were extrapolated by using values derived from experimental values at room temperature and a similar diffusion controlled profile.

### For 0.4M $\text{H}_2\text{SO}_4$ solution

The reaction scheme for neutral solution was applied for reproducing the primary yields in 0.4 M  $\text{H}_2\text{SO}_4$  solution. The reaction (1) in Table 1 was introduced for simulating the primary yields in 0.4 M  $\text{H}_2\text{SO}_4$  solution, applying the rate constant at 25°C obtained from the simulation which showed agreement with the experimentally obtained data for  $\text{G}_{\bullet\text{OH}}$  at this solution.

The value of  $1.331 \times 10^9 \text{m}^2 \text{s}^{-1}$  was applied for the diffusion coefficient of  $\text{HSO}_4^-$  at 25°C. The closest value of  $1.5 \times 10^5 \text{M}^{-1} \text{s}^{-1}$  was obtained. The temperature dependence of R1 (see Table 1) was calculated by using the Arrhenius equation,

$$k_{\text{react}} = A e^{E_{\text{act}}/RT} \quad (1)$$

where  $k_{react}$  is the rate constant of the reaction without influenced by diffusion,  $E_{act}$  is the apparent activation energy ( $\text{kJ mol}^{-1}$ ),  $A$  is a preexponential factor,  $R$  is a gas constant ( $\text{J K}^{-1} \text{mol}^{-1}$ ) and  $T$  is a temperature (K).

**Table 1.** Main reactions studied by Monte-Carlo simulations at temperatures up to  $325^\circ\text{C}$ .

Symbol	Reaction
R1	$\cdot\text{OH} + \text{HSO}_4^- \rightarrow \text{H}_2\text{O} + \text{SO}_4^{\cdot-}$
R2	$\text{H}^+ + e_{aq}^- \rightarrow \text{H}^\cdot$
R3	$\text{H}^+ + \text{OH}^- \rightarrow \text{H}_2\text{O}$
R4	$e_{aq}^- + \text{H}^\cdot \rightarrow \text{H}_2 + \text{OH}^-$
R5	$e_{aq}^- + e_{aq}^- \rightarrow \text{H}_2 + 2\text{OH}^-$
R6	$e_{aq}^- + \cdot\text{OH} \rightarrow \text{OH}^-$
R7	$e_{aq}^- + \text{H}^+ \rightarrow \text{H}^\cdot$
R8	$e_{aq}^- + \text{H}_2\text{O} \rightarrow \text{H}^\cdot + \text{OH}^-$
R9	$\text{H}^\cdot + \cdot\text{OH} \rightarrow \text{H}_2\text{O}^\cdot$
R10	$\cdot\text{OH} + \cdot\text{OH} \rightarrow \text{H}_2\text{O}_2$
R11	$\text{H}_2\text{O}_2 + e_{aq}^- \rightarrow \text{OH}^- + \cdot\text{OH}$
R12	$\text{H}^\cdot + \text{H}^\cdot \rightarrow \text{H}_2$

The value of  $1.8 \times 10^8 \text{ M}^{-1}\text{s}^{-1}$  and  $16.1185 \text{ kJ.mol}^{-1}$  were applied for  $A$  and  $E_{act}$ , respectively, which is reasonably proposed by Buxton *et al.*[15] that the activation energy of most solution in water is in between 10 and  $18 \text{ kJ mol}^{-1}$ . The ionic strength effect was introduced into the IONLYS-IRT code for R2, R3 and the value obtained for those rate constant at  $25^\circ\text{C}$  were  $1.12 \times 10^{10}$  and  $5.97 \times 10^{10} \text{ M}^{-1}\text{s}^{-1}$ , respectively, and has been reported elsewhere [16].

### Concentration

The changes in the initial concentration of  $\text{H}^+$  and  $\text{OH}^-$  for neutral solution were computed based on the temperature dependence of density change summarized by Elliot *et al.*[17]. The initial concentration of  $\text{H}^+$  for acid solution was  $0.4095 \text{ M}$  with little change with temperature due to density change. The initial concentration of  $\text{OH}^-$  was  $2.44 \times 10^{-14} \text{ M}$  and its temperature dependence was calculated by using the temperature change of  $K_w$ .

### Proton energy

The proton energy used for simulating  $^{60}\text{Co}$   $\gamma$ -ray irradiation was  $300 \text{ MeV}$  (LET of  $0.3 \text{ keV}/\mu\text{m}$ , which similar with LET of  $^{60}\text{Co}$   $\gamma$ -ray). The interaction of Fast Neutrons with material is

due to the reactions with water will mainly undergo as elastic collision and produce charged particle, protons as secondary, tertiary recoiled proton and so on [20]. The average loss in one collision is given by the equation (2),

$$\ln \frac{E_n}{E_0} = n \left[ \frac{(A-1)^2}{2A} \ln \frac{(A+1)}{(A-1)} - 1 \right] \quad (2)$$

where  $A$  is the atomic weight of struck atom, where for proton  $A=1$ ,  $E_0$  is the initial neutron energy and  $E_n$  is a neutron energy after  $n$  collisions. The final yields for fast neutrons irradiation ( $G_x$ ) are calculated by using equation (3),

$$G_x = \frac{\sum_1^n (G_{xp} E_p)}{E_T} \quad (3)$$

where  $G_{xp}$  is primary yields obtained by using one energy of recoiled proton produced by collision ( $n$ ),  $E_p$  is energy for recoiled proton produced by collision ( $n$ ) and  $E_T$  is the sum of all recoiled proton energy. The proton energies of 1.264, 0.465, 0.171, 0.063 and 0.024 MeV (corresponding to an average LET of 22, 42, 69, 76 and 59  $\text{keV}/\mu\text{m}$ , respectively) were used for simulating 2 MeV fast neutrons, and proton energies of 0.505, 0.186, 0.069 and 0.025 MeV (corresponding to an average LET of 40, 67, 76 and 60  $\text{keV}/\mu\text{m}$ , respectively) for 0.8 MeV fast neutron irradiation.

## RESULTS AND DISCUSSION

### Neutral water

#### $^{60}\text{Co}$ $\gamma$ -radiolysis

Monte Carlo simulations were used to investigate the effect of temperatures (25 to  $325^\circ\text{C}$ ) on the primary yields (g-values) of the radical and molecular products by  $^{60}\text{Co}$   $\gamma$ -ray irradiation in neutral water. The results of this study show a similar profile and good agreement with the previous study results [1].

#### 2 MeV fast neutron radiolysis

The same method as used for the  $^{60}\text{Co}$   $\gamma$ -radiolysis study was applied to calculate the radiolysis products of neutral water as a function of temperature under 2 MeV fast neutrons irradiation. Five levels of recoiled proton energy, 1.264, 0.465, 0.171, 0.063 and 0.024 MeV were simulated. The sixth level energy of recoiled proton (lower than 0.024 MeV) had little contribution to the mean final

g-values, therefore, not considered in this study. The yields of each proton energy level were obtained. From the results, it is known that except for  $g(\text{H}_2\text{O}_2)$  that stays constant, the yields increase with temperature in all cases for both simulated and experimental data [18-21].

### 0.8-MeV fast neutrons radiolysis

The simulation results show good agreement between the computed data and the experimental data [22], verifying that the yields increase with the temperature rise in all cases (Fig. 1).

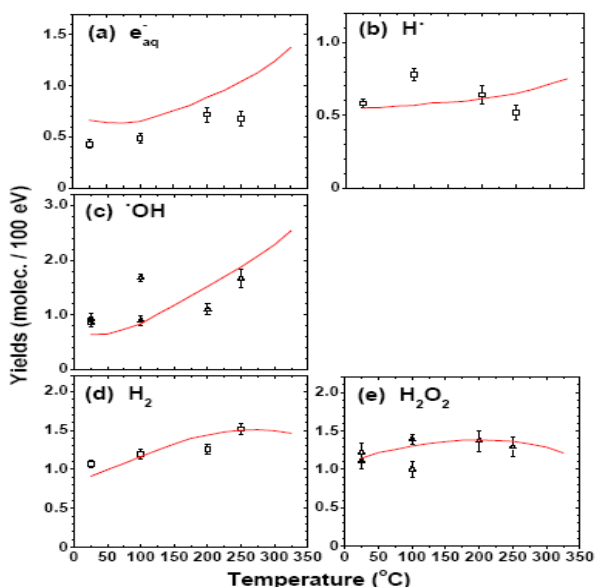


**Fig. 1.** Variation of g-values for the 0.8 MeV fast neutrons radiolysis of neutral water as a function of temperature. The simulated results obtained at  $10^{-7}$ s (—). Experimental results are from (▲)  $\text{HClO}_4$ +Methanol solutions, (Δ)  $\text{NaNO}_2$  solutions, (□) all solutions ref. [22].

The main reaction that destroyed  $e_{aq}^-$  in this simulation is the same, in principle, as that for 2 MeV fast neutron irradiations, but in different magnitude due to the LET effect.  $e_{aq}^-$  is mainly destroyed by  $^{\bullet}\text{OH}$  (R6) at 25°C but the reaction with  $\text{H}^{\bullet}$  (R7) becomes dominant at higher temperatures up to 325°C. Computed  $g(\text{H}^{\bullet})$  increases slightly with temperature (Fig. 1.b).  $g(\text{H}^{\bullet})$  is mainly destroyed by the reaction with  $^{\bullet}\text{OH}$  (R9) at 25°C. The increase in temperature will decrease  $\Delta G$  of R9. The contribution of the reaction with  $e_{aq}^-$  (R4) plays as secondary role at 25°C, but its  $\Delta G$  increase with temperature rises. Finally, R4 plays as dominant reaction in destroying  $g(\text{H}^{\bullet})$ , dwarfing the effect of R9 at 325°C.  $g(^{\bullet}\text{OH})$  also shows sharp increases

with temperature and shows good agreement with the experimental (Fig. 1.c).

Computed  $g(\text{H}_2\text{O}_2)$  gives higher values at temperatures up to 150°C (Fig. 1.e), but declines afterwards and shows also good agreement with the experimental data. The simulated results have demonstrated that radicals prefer to diffuse out from the spur at higher temperatures than react with each other. The higher LET will give a more dense spur called cylindrical spur, whereas lower LET gives spherical spurs [23-24]. At high LET, the track initially comprises a “core” of dense ‘penumbra’ consisting of dense ionization and excitations. The secondary electrons are ejected out of the core [25-26], and make it unpredictable as to when the species become homogeneously distributed in the solution. Furthermore, the accuracy of the temperature dependencies of the reactions rate constants and diffusion coefficients introduced in the calculations can not be verified because of insufficient experimental data, especially for high temperatures and high LET. In conclusion, this study produced a series of simulated results that show good agreement with the experimental data for all cases studied using neutral water irradiated by  $^{60}\text{Co}$   $\gamma$ -rays and fast neutrons 2 and 0.8 MeV.

### 0.4 M $\text{H}_2\text{SO}_4$ solutions

#### $^{60}\text{Co}$ $\gamma$ -radiolysis

In general, all simulated results in this study show good agreement with the experimental data by Hohanadel and Ghormley (1962) and Kabakchi *et al.* (1987) up to 100°C, however Kabakchi *et al.* show consistently higher values and also the increase with temperature. Figure 2 Katsumura *et al.* show lower values from 100 to 250°C but the computed data are shown to be within tolerance of their experimental errors.

The experimental values of  $g(\text{H}_2)$  obtained by Hohanadel and Ghormley (1962) are in good agreement and also with Katsumura *et al.* (1988) and Kabakchi (1987) (Fig. 2.d).  $g(\text{H}_2)$  in acidic solutions is mainly formed by self-reaction of  $\text{H}^{\bullet}$  (R12) and become dominant at entire temperatures, followed by reaction of  $\text{H}^{\bullet}$  with  $e_{aq}^-$  (R4) and then self-reaction of  $e_{aq}^-$  (R5). The increase temperatures will expedite the  $\Delta G$  of R4 and R5.

The  $g(^{\bullet}\text{OH})$  values obtained by these 3 authors are in good agreement with the simulated values in this study up to 200°C as shown in Fig. 2.c. However, Kabakchi *et al.* (1986) show higher values at 250°C but within the tolerance of

error. The increase in temperature will slow down the increasing of  $g(\cdot\text{OH})$ . The main species that destroy  $\cdot\text{OH}$  in acid solutions is  $\text{HSO}_4^-$  (R1), which becomes dominant at higher temperatures.

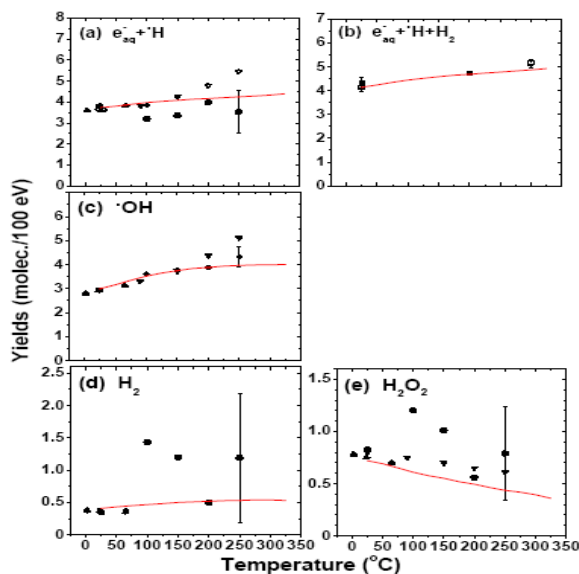


**Fig. 2.** Variation of  $g$ -values for the  $\gamma$ -rays radiolysis of  $0.4\text{ M H}_2\text{SO}_4$  solutions as a function of temperature. The simulated results obtained at  $10^{-7}\text{ s}$  (—). Experimental results are from ( $\blacktriangle$ ) ref. [27], ( $\circ$ ) ref. [28], ( $\blacktriangledown$ ) ref. [29], ( $\bullet$ ) ref. [30] and ( $\blacksquare$ ) from  $\text{H}_2$  measurement ( $\square$ ), from Ferric ions measurement ref. [31].

$g(\text{H}_2\text{O}_2)$  decreases with the temperature rises and show good agreement with the experimental data obtained by Hochanadel and Ghormley (1962), and Katsumura *et al.* (1988) (Fig. 2.e). It should be noted, however, that their experimental values have relatively high tolerance of error at high temperatures. Kabakchi and Ghormley show data with good agreement with this study but with slightly elevated values at high temperatures.

The main destroying reaction of  $\text{H}_2\text{O}_2$  by  $e_{aq}^-$  (R11) only significant for neutral water at  $25^\circ\text{C}$  and become negligible for higher temperatures and acidic solutions. Therefore, the  $g(\text{H}_2\text{O}_2)$  for both solutions gives similar value at  $325^\circ\text{C}$ . This study has demonstrated that the process in acid solutions under  $^{60}\text{Co}$   $\gamma$ -rays can also be successfully simulated by Monte-Carlo code.

### 0.8 MeV fast neutron radiolysis

Figure 3 shows the simulated results together with the only one set of available experimental value obtained by Katsumura *et al.* (1992) [32]. This profile of computed sum of reducing species of  $e_{aq}^-$  and  $\text{H}^\bullet$  is different to the experimental results,

which show the increase with temperature. On the contrary,  $g(\text{H}_2)$  decreases with temperature, although the simulated results show good agreement up to  $50^\circ\text{C}$  (Fig. 3.c.). Similar with that for  $^{60}\text{Co}$   $\gamma$ -ray irradiation in acidic solutions, the formation of  $\text{H}_2$  under 0.8 MeV fast neutron irradiation is mainly due to the self-reaction of  $\text{H}^\bullet$  (R12) with a small contribution from the R4 and R5. The computed  $g(\cdot\text{OH})$  data increase with temperature and are in good agreement with the experimental data (Fig. 3.b.). A similar profile but with different magnitude to the experimental data was obtained from this study, whereas  $g(\text{H}_2\text{O}_2)$  is shown to decrease with temperature (Fig. 3.d.).

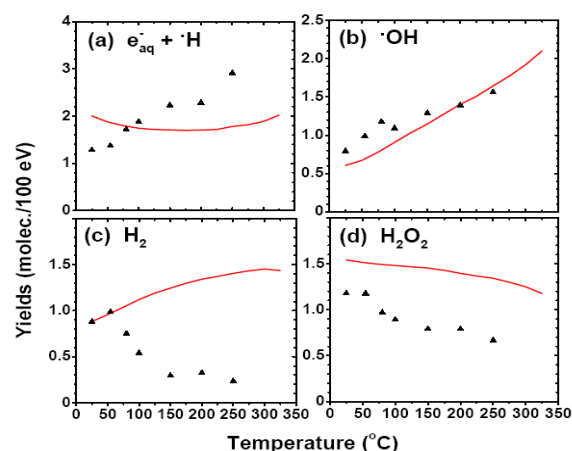


**Fig. 3.** Variation of  $g$ -values for the 0.8 MeV fast neutrons radiolysis of  $0.4\text{ M H}_2\text{SO}_4$  as a function of temperature. The simulated results obtained at  $10^{-7}\text{ s}$  (—). Experimental results are from from ( $\blacktriangle$ ) ref. [32].

Compared with the  $^{60}\text{Co}$   $\gamma$ -ray irradiation result for the acid solution, it is demonstrated that the 0.8 MeV fast neutron radiolysis gives higher molecular products of  $\text{H}_2$  and  $\text{H}_2\text{O}_2$ , and the lower radical product of  $\text{H}^\bullet$ ,  $e_{aq}^-$  and  $\cdot\text{OH}$  because of the LET effect. This study shows that the highly concentrated  $\text{H}^+$  in the solution raises the number of  $\text{H}_2\text{O}_2$  by factor of 1.5 at  $25^\circ\text{C}$  that different with that on  $^{60}\text{Co}$   $\gamma$ -radiolysis that only gives little changes. As compare with the computed  $^{60}\text{Co}$   $\gamma$ -radiolysis, due to higher LET, the  $\Delta G$  formation of  $\text{H}_2\text{O}_2$  for 0.8 MeV fast neutron is higher than that for  $^{60}\text{Co}$   $\gamma$ -radiolysis at  $25^\circ\text{C}$ , and decrease steeply with temperature rises. As mentioned above that the destroying reaction of  $\text{H}_2\text{O}_2$  by  $e_{aq}^-$  (R11) for acid solutions is insignificant for both  $^{60}\text{Co}$   $\gamma$ -ray and fast neutron irradiation. For acidic solutions, the temperature dependence profiles of computed  $g(\cdot\text{OH})$  for  $^{60}\text{Co}$   $\gamma$ -radiolysis increases from 2.8 to 4, at 25 to  $325^\circ\text{C}$ , and for 0.8 MeV fast neutron

radiolysis, a big increases from about 0.6 to 2.1, at 25 to 325°C. Computed  $g(\text{H}_2\text{O}_2)$  for  $^{60}\text{Co}$   $\gamma$ -radiolysis decreases from about 0.7 to 0.36, at 25 to 325°C, and for fast neutrons decreases from about 1.55 to 1.25, at 25 to 325°C.

The temperature dependence profiles of  $g(\text{H}_2)$  and  $g(e_{aq}^- + \text{H}^\bullet)$  for both  $^{60}\text{Co}$   $\gamma$ -rays and 0.8 MeV fast neutron irradiation are different. The  $g(\text{H}_2)$  temperature dependence for  $^{60}\text{Co}$   $\gamma$ -radiolysis is constant, showing little changes with temperature. However, for 0.8 MeV fast neutron irradiation, it increases from about 0.88 to 1.45, at 25 to 325°C. The  $g(e_{aq}^- + \text{H}^\bullet)$  temperature dependence for  $^{60}\text{Co}$   $\gamma$ -ray irradiation increases, whereas the 0.8 MeV fast neutrons have little effect.

Compare with that for neutral water under 0.8 MeV fast neutron irradiation, simulated  $g(e_{aq}^- + \text{H}^\bullet)$  for acid solutions raised by factor of almost two at 25°C, and becomes a little lower at 325°C. The presence of acid gives little lower value of  $g(\text{H}_2)$  for acidic solutions at whole temperature ranges compare with that for neutral water. The value of  $g(\bullet\text{OH})$  for both solutions are the same at 25°C and lower value at 325°C than that for neutral water.  $g(\text{H}_2\text{O}_2)$  for acidic solutions give a higher value at 25°C and little lower or almost similar value at 325°C compare with that for neutral water.

The general profile of the simulated temperature effect in this study clearly illustrates that except for  $g(\text{H}_2)$  that almost constant or little increases,  $g$ -values of radicals increase with temperature rises and  $g(\text{H}_2\text{O}_2)$  almost constant or decrease for both neutral and acidic solutions under  $^{60}\text{Co}$   $\gamma$ -rays or higher LET irradiation. The presence of acid gives similar tendencies for both  $^{60}\text{Co}$   $\gamma$ -rays and 0.8-fast neutron irradiation, but in different magnitude. However, as mentioned above, the experimental data for acidic solutions under 0.8 MeV fast neutrons give the opposite results with the computed data for  $g(\text{H}_2)$  and  $g(\text{H}^\bullet)$ , rendering the understand on radiolytic products behavior of little value to this study. It is suggested that more experimental data under fast neutron irradiation are needed to better understand the behaviors of radiolytic products for both solutions.

## CONCLUSION

Monte-Carlo simulations were used to study the behavior of radiolysis products for neutral water and 0.4 M  $\text{H}_2\text{SO}_4$  solution, at temperatures from 25 to 325°C under  $^{60}\text{Co}$   $\gamma$ -rays and fast neutrons of

2 and 0.8 MeV. The results were compared to the available experimental data. This work produced a series of simulated results showing good agreement with the experimental data for all cases studied except for the acid solution with 0.8 MeV fast neutron irradiation. Except for  $g(\text{H}_2\text{O}_2)$ , all the radicals and molecular products increase with the temperature rises. Fast neutron irradiation gives the higher molecular products and lower radicals than that for  $^{60}\text{Co}$   $\gamma$ -ray irradiation. In  $^{60}\text{Co}$   $\gamma$ -radiolysis, except for  $g(\text{H}_2)$  that gives lower value at 25°C and higher value at 325°C, the presence of acid gives the higher values for radicals and  $g(\text{H}_2\text{O}_2)$  at 25°C and lower values at 325°C, compared with that for neutral water. The fast neutron radiolysis on acidic solutions was demonstrated by the simulation, that gives similar tendencies with that for  $^{60}\text{Co}$   $\gamma$ -radiolysis. More experimental data under fast neutron irradiation are needed for better understand the behavior of radiolytic product, especially under acidic conditions.

## REFERENCES

1. M.A. Hervé du Penhoat, T. Goulet, Y. Frongillo, M.-J. Fraser, Ph. Bernat and J.-P. Jay-Gerin, *J. Phys. Chem. A* **104** (2000) 11757.
2. M.A. Hervé du Penhoat, J. Meesungnoen, Thomas T. Goulet, Y. Frongillo, A. Filali-Mouhim, S. Mankhetkorn and J.-P. Jay-Gerin, *Chem. Phys. Lett.* **341** (2001) 135.
3. V. Cobut, Y. Frongillo, J.-P. Jay-Gerin and J.P. Patau, *J. Chim. Phys.* **91** (1994) 1018.
4. Y. Frongillo, M.-J. Fraser, V. Cobut, T. Goulet, J-P Jay Gerin and J.P. Patau, *J. Chem. Phys.* **93** (1996) 93.
5. V. Cobut, Y. Frongillo, J.P. Patau, T. Goulet, M.-J. Fraser and J-P Jay Gerin, *Radiat. Phys. Chem.* **51** (1998) 229.
6. Y. Frongillo, T. Goulet, M.-J. Fraser, V. Cobut, J.P. Patau and J-P Jay Gerin, *Radiat. Phys. Chem.* **51** (1998) 245.
7. T. Goulet, M.-J. Fraser, Y. Frongillo and J.-P. Jay-Gerin, *Radiat. Phys. Chem.* **51** (1998) 85.
8. P. Clifford, N.J.B. Green, M.J. Pilling and S.M. Pimblott, *J. Phys. Chem.* **90** (1987) 4417.
9. N.J.B. Green, M.J. Pilling, S.M. Pimblott and P. Clifford, *J. Phys. Chem.* **90** (1990) 251.

10. S.M. Pimblott, M.J. Pilling and N.J.B. Green, *Radiat. Phys. Chem.* **37** (1991) 377; J. Meesungnoen and J.-P. Jay-Gerin, *J. Phys. Chem. A* **109** (2005) 6406.
11. J.W.T. Spinks and R.J. Woods, *An Introduction to Radiation Chemistry*, Third Edition (1990).
12. T. Goulet and J.-P. Jay-Gerin, *J. Phys. Chem.* **92** (1998) 6871.
13. T. Goulet and J.-P. Jay-Gerin, *Radiat. Res.* **118** (1989) 46.
14. T. Goulet, J.P. Patau and J.-P. Jay-Gerin, *J. Phys. Chem.* **94** (1990) 7312.
15. G.V. Buxton, N. Wood. and S. Dyster, *J. Chem. Soc. Faraday Trans. I.* **84** (1988) 1113.
16. J. Meesungnoen, M. Benrahmoune, A. Filali-Mouhim, S. Manketkorn and J.-P. Jay-Gerin, *Radiat. Res.* **155** (2001) 269.
17. A.J. Elliot, AECL-11073, COG-94-167, October (1994).
18. G.V. Buxton, C.L. Greenstock, W.P. Helman and A.B. Ross, *J. Phys. Ref. Data* **17** (1998) 513.
19. W.G. Burns and P.B. Moore, *Radiat. Effects* **30** (1976) 233.
20. H. Christensen, A. Molander, A. Lassing and H. Tomani, *Water Chemistry of Nuclear Reactor Systems 7*, BENS (1996).
21. A.J. Elliot, M.O. Chenier, D.C. Quellette and V.T. Koslowsky, *J. Phys. Chem.* **100** (1996) 9014.
22. A.J. Elliot, M.P. Chenier and D.C. Quellette, *J. Chem. S.C. Faraday Trans.* **89** (1993) 1193.
23. S. Gordon, K.H. Schmidt and J.R. Honekamp, *Radiat. Phys. Chem.* **21** (1983) 247.
24. J.W.T. Spinks and R.J. Woods, *Introduction to Radiation Chemistry*, 3<sup>rd</sup> ed., Wiley, New York (1990) 243.
25. J.L. Magee and A. Chatterjee, *Track Reactions of Radiation Chemistry*, in: *Kinetics of Non-Homogeneous Processes*, G.R. Freeman (Ed.), Wiley, New York (1987) 171.
26. A. Mozumder, *Fundamentals of Radiation Chemistry*, Academic Press, San Diego, CA (1999) 41.
27. C.J. Hochanadel and J.A. Ghormley, *Radiat. Res.* **16** (1962) 653.
28. S.A. Kabakchi and I.E. Lebedeva, *High Energy Chem.* **20** (1986) 307.
29. S.A. Kabakchi and I.E. Lebedeva, *High Energy Chem.* **21** (1987) 261.
30. Y. Katsumura, Y. Takeuchi, and K. Ishigure, *Radiat. Phys. Chem.* **32** (1988) 259.
31. A.J. Elliot, D.C. Quellette, D. Reid and D.R. McCracken, *Radiat. Phys. Chem.* **34** (1989) 747.
32. Y. Katsumura, D. Yamamoto, D. Hiroishi and K. Ishigure, *Radiat. Phys. Chem.* **39** (1992) 383.